

SCIENTIFIC REPORTS

OPEN

Influence of p53 Isoform Expression on Survival in High-Grade Serous Ovarian Cancers

Katharina Bischof^{1,2}, Stian Knappskog^{3,4}, Sigrun M. Hjelle^{1,7}, Ingunn Stefansson^{5,6}, Kathrine Woie², Helga B. Salvesen^{1,2}, Bjorn T. Gjertsen^{1,7} & Line Bjorge^{1,2}

High-grade serous ovarian carcinoma (HGSOC) is characterised by alterations in the p53 pathway. The expression levels of p53 isoforms have been shown to be associated with patient survival in several cancers. This study examined the predictive and prognostic effects of the expression levels of *TP53* pre-mRNA splicing isoforms and *TP53* mutations in tumour tissues in 40 chemotherapy responders and 29 non-responders with HGSOC. The mRNA expression levels from total p53, and total $\Delta 133p53$, p53 β , p53 γ isoforms were determined by RT-qPCR, and *TP53* mutation status by targeted massive parallel sequencing. The results from these analyses were correlated with the clinical outcome parameters. No differential expression of p53 isoforms could be detected between the chemosensitive and chemoresistant subgroups. In a multivariate Cox regression model, high levels of total $\Delta 133p53$ were found to be an independent prognosticator for improved overall survival (HR = 0.422, $p = 0.018$, 95% CI: 0.207–0.861) and reached borderline significance for progression-free survival (HR = 0.569, $p = 0.061$, 95% CI: 0.315–1.027). *TP53* mutations resulting in loss of function or located at known hotspots were predictive of tumour characteristics and disease progression. These findings suggest that total $\Delta 133p53$ mRNA can be a biomarker for survival in HGSOC.

Mutations in the *TP53* gene are early and almost ubiquitous events in the genesis of high-grade serous ovarian carcinoma (HGSOC)^{1–4}. Although various classes of mutations occur throughout the coding region of the *TP53* gene in human cancers, there is a clear enrichment of missense or nonsense single base substitutions affecting the DNA-binding domain of the protein⁵. Since large-scale sequencing data for *TP53* mutations became available, the predictive and prognostic roles of defined subcategories of *TP53* mutations have been extensively investigated. Alterations that result in a loss of function (LOF) or oncogenic mutations conferring to tumour-promoting abilities have been shown to be associated with chemoresistance and worse survival in ovarian cancers^{6–9}. Small molecule therapies targeting mutated p53 proteins in cancer cells are under development for the treatment of ovarian cancer and may lead to *TP53* mutational guided therapy^{10,11}.

In humans, the *TP53* gene encodes RNA that is edited by pre-mRNA splicing, yielding at least 12 protein isoforms expressed to various degrees in different tissues and under various physiological conditions¹² (Fig. 1). Emerging evidence has linked the deregulated expression of these isoforms to cancer^{13–18}. The amino-terminally truncated $\Delta 133p53$ isoform is the product of alternative promoter usage and has been shown to exert dominant-negative functions toward canonical p53 in colon cancer cell line models¹⁸. In addition, $\Delta 133p53$ has been shown to inhibit replicative senescence and to promote cellular proliferation¹³. The biological role of the carboxy-terminally truncated p53 β and p53 γ isoforms, both products of alternative splicing of intron 9^{18–20}, is still being debated. However, these isoforms have been shown to enhance p53's tumour-suppressive transcriptional activity of Bax and p21^{21,22}.

¹Centre for Cancer Biomarkers CCBIO, Department of Clinical Science, University of Bergen, 5020, Bergen, Norway.

²Department of Gynecology and Obstetrics, Haukeland University Hospital, 5021, Bergen, Norway. ³Department of Oncology, Haukeland University Hospital, 5021, Bergen, Norway. ⁴Section of Oncology, Department of Clinical Science, University of Bergen, 5020, Bergen, Norway. ⁵Department of Pathology, Haukeland University Hospital, 5021, Bergen, Norway. ⁶Centre for Cancer Biomarkers CCBIO, Department of Clinical Medicine, Section for Pathology, University of Bergen, 5020, Bergen, Norway. ⁷Department of Internal Medicine, Haematology Section, Haukeland University Hospital, 5021, Bergen, Norway. Helga B. Salvesen is deceased. Correspondence and requests for materials should be addressed to L.B. (email: line.bjorge@uib.no)

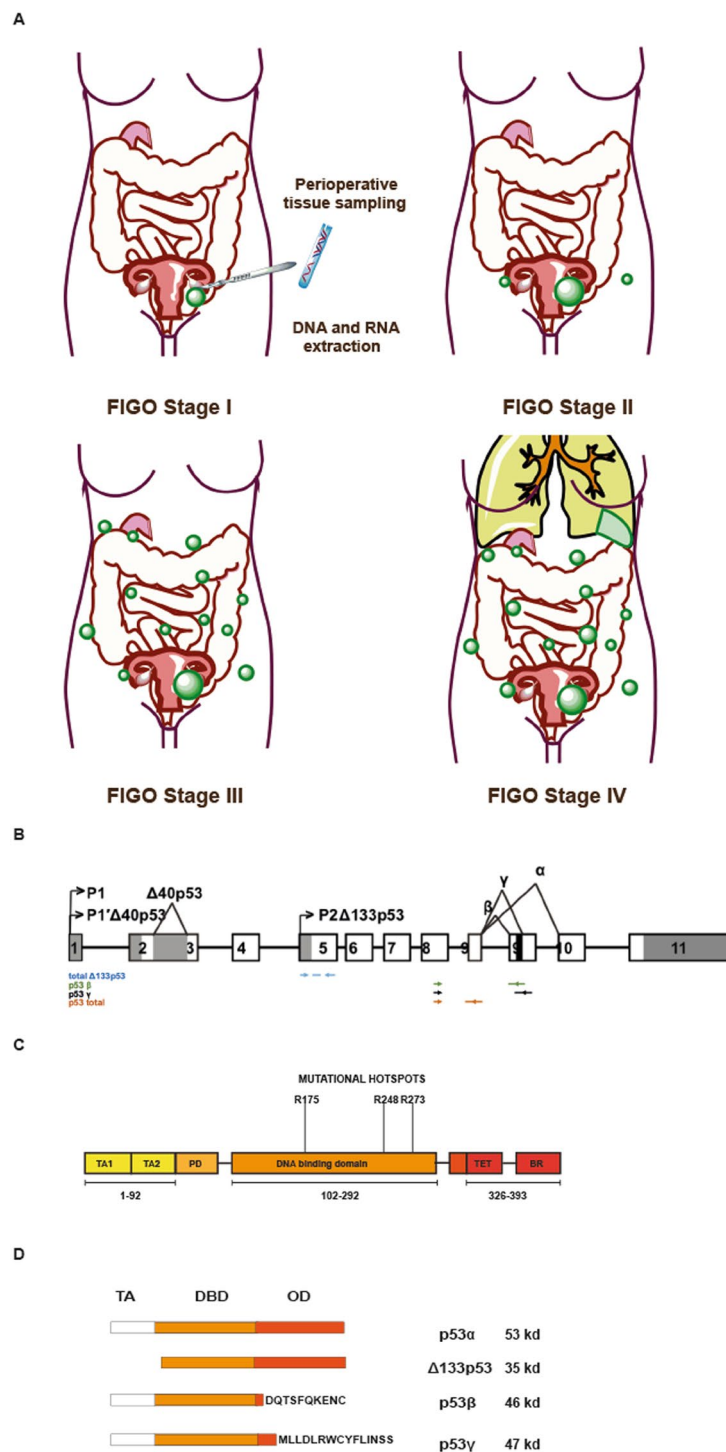


Figure 1. (A) Overview of FIGO disease stages represented by the series for this study and illustration of sample collection and extraction of DNA and RNA. (B) Structure of the human TP53 gene comprising 11 exons. P1 = proximal promoter encoding full-length p53, P2 = internal promoter resulting in $\Delta 133p53$ product. Alternative splicing sites (\wedge). Primer location is indicated by coloured arrows and is indexed on the lower left. (C) Provides a more detailed schematic illustration of the distinct functional and structural domains of the 393 amino acid long p53 protein. TA1 and TA2 form the transactivation domain, followed by the proline rich domain (PD) and the DNA binding domain, where the three most frequently found point mutations in high-grade serous gynaecological cancers are indicated. The tetramerization domain (TET) and basic region (BR) form the C-terminus. (D) Illustrates the exon composition of canonical p53 and relevant p53 isoforms. Abbreviations: Transactivation domain (TA), DNA binding domain (DBD), C-terminal oligomerization domain (OD). The N-terminally truncated isoform $\Delta 133p53$ is a product of the regulation of an internal promoter in intron 4 (P2). The C-terminally altered p53 β and p53 γ isoforms have alternative sequences after amino acid 332. Molecular weight indicated in kilodalton (kd) on the right side.

Clinical parameters	Poor response	Good response
	Mean (range)	Mean (range)
Age at diagnosis; in years	59 (31–75)	61 (44–77)
Time to progression; in months	3 (1–6)	42 (17–137)
	N (%)	N (%)
Tumor grade		
Grade 2	8 (28%)	7 (17%)
Grade 3	21 (72%)	33 (83%)
FIGO stage		
IIIC	21 (72%)	36 (90%)
IV	8 (28%)	4 (10%)
Macroscopic surgical resection (data missing for 5 respectively 8 cases)		
Complete	—	16 (50%)
Residual disease ≤1 cm	16 (67%)	12 (38%)
Residual disease >1 cm	8 (33%)	4 (12%)

Table 1. Distribution of clinicopathologic characteristics for 69 patients within subgroups of high grade FIGO stages \geq IIIC enriched for either good response; ≥ 17 months progression free survival after completed primary treatment (surgery followed by adjuvant chemotherapy) or poor response with disease progression within 6 months after completed primary treatment.

Previous studies, including those by the authors, have reported that in gynaecological malignancies, such as epithelial ovarian cancers and uterine serous cancers, the altered expression of the p53 isoforms was associated with tumour traits, such as grade of differentiation, sensitivity to chemotherapy and survival^{23–26}.

Chemotherapy resistance remains a major obstacle in the successful treatment of patients with HGSOC. Data from high-resolution copy-number profiles on tumour samples collected throughout therapy indicate that HGSOC already exhibits substantial clonal diversity at primary diagnosis²⁷; therefore, the high rates of acquired chemoresistance may be a result of subset selection with primary innate chemoresistance²⁸.

In the current study, we aimed to investigate the predictive and prognostic impact of the p53 isoforms in a cohort of HGSOC patients selected based on their response or non-response to chemotherapy. The potential predictive and prognostic roles were explored based on the mRNA expression levels of the individual *TP53* isoforms in HGSOC tumour tissue (Fig. 1C). High mRNA levels of the amino-terminal altered total $\Delta 133p53$ isoform were associated with favourable survival. These findings suggest the total $\Delta 133p53$ isoform to be a possible biomarker for disease progression in HGSOC, worthy of further validation.

Results

Prognostic value of clinical characteristics. The sample in the present study comprised 69 patients with HGSOC. These 69 cases were selected from a cohort of 493 epithelial ovarian cancers (EOCs) (see Methods section) based on their poor ($n = 29$) responses or good ($n = 40$) responses to adjuvant treatment with carboplatin and taxane, thus representing chemoresistant and chemosensitive subsets, respectively. A poor response to adjuvant therapy was defined as disease progression after ≤ 6 months after completed primary platinum/taxane based chemotherapy, and a good response was ≥ 17 months of progression-free survival (PFS). The mean age at the time of diagnosis was 59 (range 31–75) for poor responders and 61 (range 44–77) for good responders. It was noted that 72% (21 of 29) of the poor responders presented with International Federation of Gynecology and Obstetrics (FIGO) stage IIIC disease at the time of primary treatment, and 90% (36 of 40) of good responders were diagnosed at stage IIIC. In both cohorts, a majority of the tumours exhibited high-grade differentiation (see Table 1.)

Univariate and multivariate Cox regression analyses (see Table 2) were performed to determine the prognostic relevance of the clinicopathological prognosticators in the combined sample set ($n = 69$), and disease stage was found to be a predictor of PFS (univariate analysis [$p = 0.007$]; multivariate analysis [hazard ratio = 2.317, $p = 0.033$, 95% CI: 1.071–5.012]). The results of the univariate analysis showed disease stage to be significantly associated with overall survival (OS), ($p = 0.002$), and the results of the multivariate model showed borderline significance (hazard ratio = 2.299, $p = 0.051$, 95% CI: 0.998–5.297). The presence of residual disease after surgery also had an effect on PFS, as seen in the univariate risk model ($p = 0.032$), and OS, as seen in the univariate analysis ($p = 0.017$) and the multivariate analysis (hazard ratio = 3.735, $p = 0.041$, 95% CI: 1.054–13.240). Other clinicopathological variables, such as patient age and tumour grade, had no significant effect on the survival parameters.

mRNA levels of p53 isoforms in HGSOC. The levels of the total p53 mRNA were quantified, and breakpoint-specific qPCR assays were applied to detect the amino-terminal truncated total $\Delta 40p53$ and total $\Delta 133p53$ isoforms, and the carboxy-terminal truncated p53 β and p53 γ isoforms. Thus, the levels of the p53 transcripts containing each of the breakpoints, but not the combined mRNA species (e.g. $\Delta 133p53\beta$ and $\Delta 133p53\gamma$) could be quantified. We identified the p53 isoforms total $\Delta 133p53$ and the splice isoforms p53 β and p53 γ in all but one of the samples (68 of 69); however, the expression levels of the total $\Delta 40p53$ mRNA could not be traced in any of the analysed samples. The landscape of the p53 isoforms was dominated by total $\Delta 133p53$ isoforms, which

	Progression-free survival Multivariate			Overall survival Multivariate		
	Univariate P-value	HR (95% CI)	P-value	Univariate P-value	HR (95% CI)	P-value
Age at diagnosis; in years	0.557	0.994 (0.958–1.032)	0.77	0.257	0.976 (0.934–1.021)	0.292
Disease stage III vs. IV	0.007	2.317 (1.071–5.012)	0.033	0.002	2.299 (0.998–5.297)	0.051
Tumor grade II vs. III	0.65	0.843 (0.411–1.731)	0.643	0.956	1.135 (0.456–2.826)	0.785
Residual disease 0 vs >0	0.032	1.810 (0.830–3.950)	0.136	0.017	3.735 (1.054–13.240)	0.041

Table 2. Established, clinical prognosticators for survival in univariate and multivariate Cox regression analysis in 69 patients with HGSO. Abbreviations: HR = Hazard ratio. CI = Confidence interval.

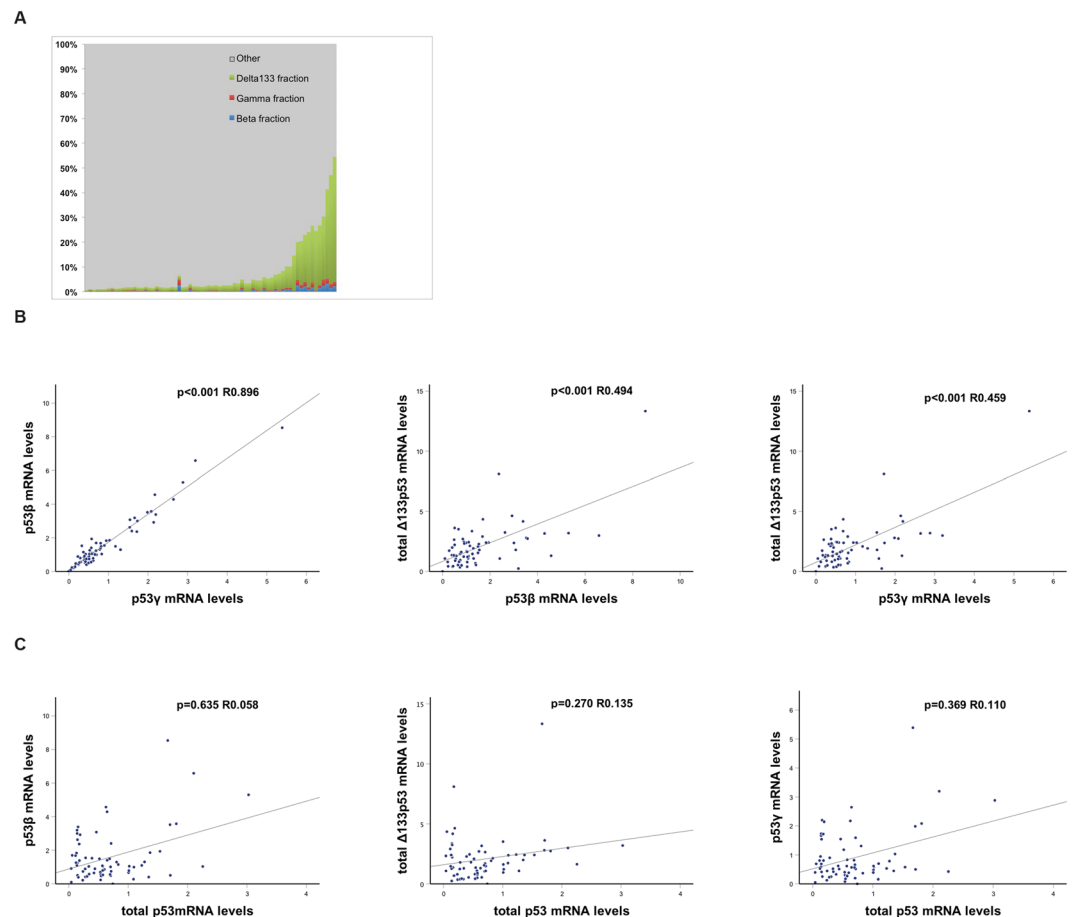


Figure 2. mRNA expression of p53 isoforms in tumour samples illustrated as (A). Histogram displaying fractions of p53 isoforms to total p53 mRNA in individual specimens. (B) Expression of p53 isoforms between each other; p53 γ versus p53 β , p53 β versus Δ 133p53, p53 γ versus Δ 133p53. (C) Expression levels of total p53, together with individual p53 β , Δ 133p53 and p53 γ isoforms.

represented up to 50.6% of the total p53 mRNA; p53 β and p53 γ accounted for a maximum of 3.3% and 2.5% of the total pool of p53 isoforms, respectively (Fig. 2A). The p53 γ isoform showed the largest variability between the lowest and the highest expressing samples (108-fold). The differences between the highest and the lowest expressing samples for the p53 β and total Δ 133p53 isoforms were 86-fold and 54-fold, respectively.

Correlation between levels of p53 isoforms and total p53. The mRNA levels of the total Δ 133p53 isoforms and the p53 β and p53 γ isoforms were all highly significantly correlated (p53 β vs. p53 γ $R = 0.896$, $p < 0.001$; p53 β vs. total Δ 133p53 $R = 0.494$, $p < 0.001$; p53 γ vs. total Δ 133p53 $R = 0.459$, $p < 0.001$; Fig. 2B). The expression levels of the individual isoforms were found to be independent of the total p53 levels ($p > 0.25$ for all of the comparisons; Fig. 2C).

Relative expression of p53 isoforms to total p53 associated with TP53 mutation status. The levels of total p53 were significantly lower in the TP53 wild-type tumours ($n = 5$) than in the mutated specimens ($n = 26$; $p = 0.036$) (Fig. 3A). While the absolute mRNA levels of the p53 isoforms were not correlated with

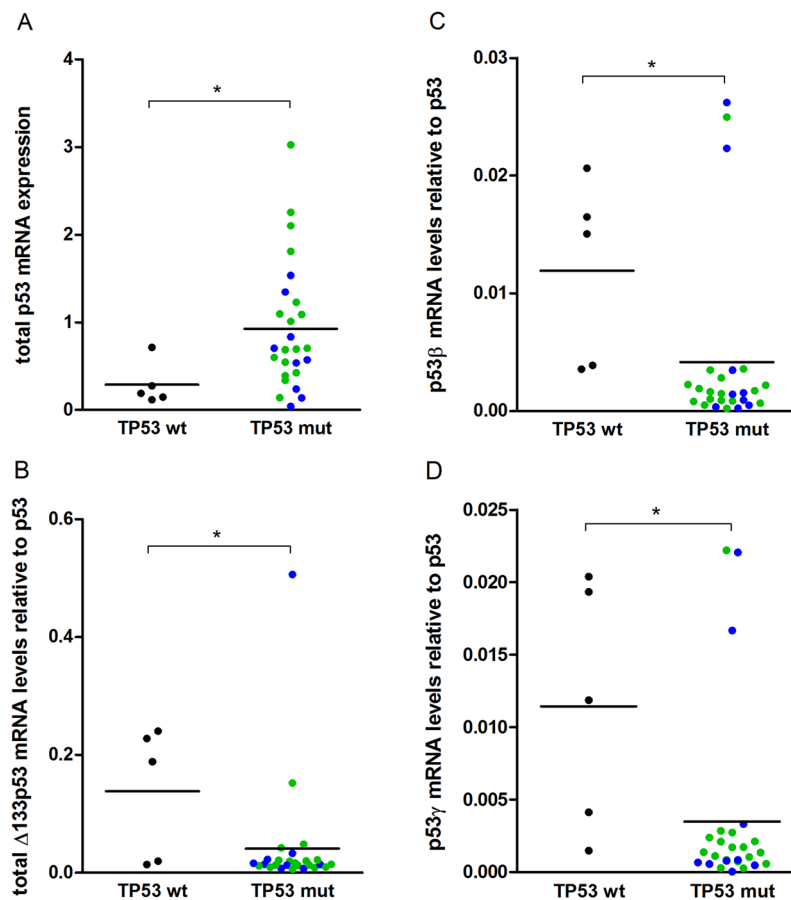


Figure 3. mRNA expression levels in individual tumour samples stratified for *TP53* mutation status for (A) Total p53 mRNA, (B) p53 β mRNA relative to total p53, (C) Δ 133p53 mRNA relative to total p53, (D) p53 γ mRNA relative to total p53. *Denotes significance level $p \leq 0.05$ blue colour indicates unclassified *TP53* mutation, green colour denominates the LOF/hot spot *TP53* mutation category.

the *TP53* mutation status, the relative expression levels of the p53 isoforms as a fraction of the total p53 levels were higher in the wild-type specimens compared to the mutated specimens (total Δ 133p53 relative to total p53 [$p = 0.036$], p53 β relative to total p53 [$p = 0.006$], p53 γ relative to total p53 [$p = 0.016$]; Fig. 3B–D).

Prognostic effect of p53 isoforms. In further analyses, the levels of each isoform and the relative level, as a fraction of the total p53 levels, were used for comparisons with the clinical parameters. In the univariate OS analysis, the relative expression of total Δ 133p53 was weakly associated with the prognosis (logrank $p = 0.173$; Fig. 4A). This association was further examined in a Cox proportional-hazards survival model. Known clinical prognostic factors for ovarian cancer patients (age at diagnosis grouped by median, tumour stage and presence of residual tumour) were introduced as binary variables, together with the relative Δ 133p53 expression grouped by median (Δ 133p53ratio high vs. low). The relative expression of total Δ 133p53 isoforms to total p53 was found to be associated with longer OS (hazard ratio = 0.422, $p = 0.018$, 95% CI: 0.207–0.861 Table 3). For the other isoforms, no prognostic role could be established in the univariate analyses (Fig. S1) or the multivariate analyses.

p53 isoforms as predictive marker for sensitivity to chemotherapy. No significant difference was observed in the expression levels of the isoforms between the two predefined groups of chemoresistant and chemosensitive patients (Δ 133p53 $p = 0.135$; p53 β $p = 0.961$; p53 γ $p = 0.496$; Mann-Whitney rank test). PFS was regarded as a surrogate marker for the efficacy of first-line chemotherapy and chemosensitivity. Higher than median levels of Δ 133p53 were not associated with significantly altered time to progression, based on the results of the univariate survival analysis using the Kaplan-Meier estimator (logrank $p = 0.216$; see Fig. 4B). In the multivariate survival analyses, the expression of Δ 133p53 grouped by median (Δ 133p53 high vs. low) reached borderline significance for PFS (hazard ratio = 0.569, $p = 0.061$, 95% CI: 0.315–1.027 Table 3). For the other isoforms, the results of the univariate analyses (Fig. S2) and the multivariate analyses showed no association between the absolute or relative expression and survival.

Associations between p53 isoform levels and clinicopathological parameters. No significant differences in the p53 isoform expression were observed between the completely resected patients and the patients

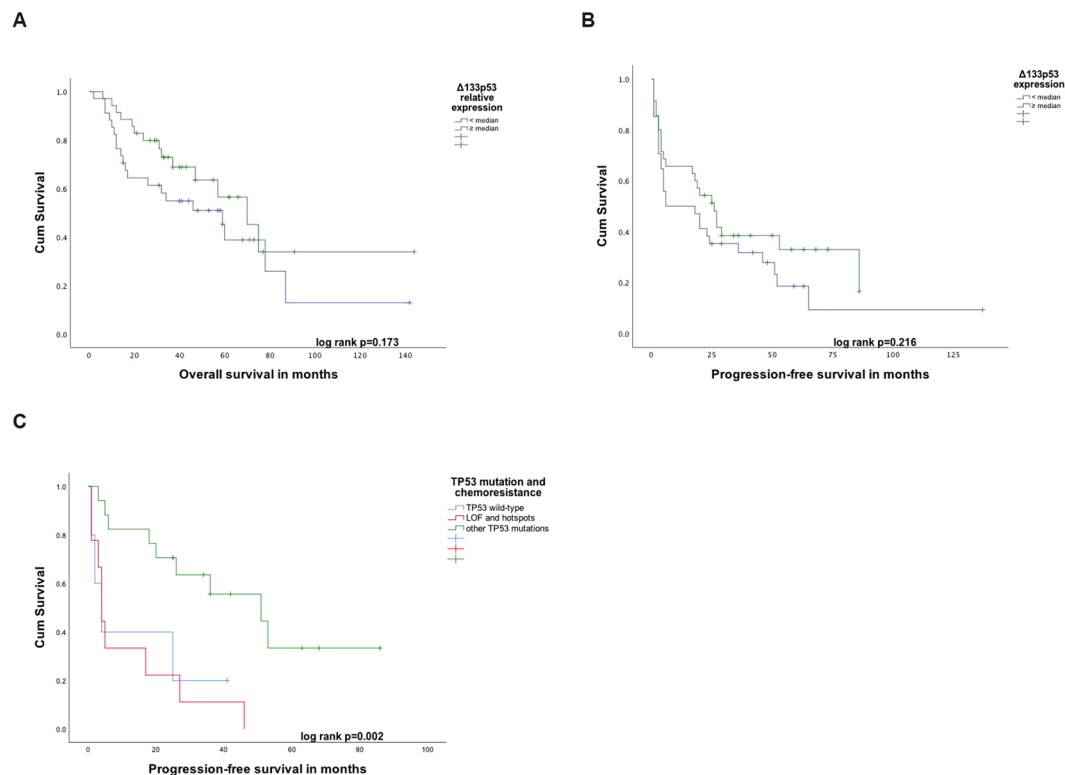


Figure 4. Kaplan-Meier survival plots for differential survival in patients expressing. (A) Higher vs. lower than median levels of $\Delta 133p53$ relative to total p53. (B) Illustration of PFS in patients, divided by median expression of $\Delta 133p53$ mRNA. (C) Kaplan-Meier survival plot for patients carrying cancers classified as *TP53* wild-type, LOF and hotspot mutations vs. other *TP53* mutations.

	Progression free survival		Overall survival	
	HR (95% CI)	P-value	HR (95% CI)	P-value
Age at diagnosis; in years	0.993 (0.956–1.031)	0.710	0.975 (0.931–1.021)	0.274
Tumor stage IIIC vs. IV	2.694 (1.259–5.765)	0.011	2.357 (1.092–5.088)	0.029
Residual disease; in cm 0 vs. >0	1.928 (0.911–4.077)	0.086	5.254 (1.481–18.642)	0.010
$\Delta 133p53$ High vs. Low	0.569 (0.315–1.027)	0.061		
High vs. Low			0.422 (0.207–0.861)	0.018

Table 3. Prognostic and predictive impact of the p53 splice variant $\Delta 133p53$ for 69 women with HGSOC in multivariate Cox regression analysis. $\Delta 133p53$ ratio denominates mRNA expression of $\Delta 133p53$ as a fraction of the total p53 levels.

for whom complete resection could not be achieved. In addition, a comparison of the moderate and low differentiated cases showed no differences in the p53 isoform levels. The expression of the p53 γ isoform was associated with age when grouped by median ($p = 0.044$); however, the expression of the other isoforms showed no association with patient age. The levels of the p53 β isoform relative to the total p53 were significantly higher expressed in the FIGO stage III vs. IV ($p = 0.05$) specimens.

Clinical relevance of *TP53* mutation status. The combined data for the *TP53* mutation status and the p53 isoform expression were available for 31 patients. The main reason for this limited number of cases was lack of access to germline DNA (needed to distinguish somatic and germline variants detected in tumour). The known *TP53* hotspot mutations, such as R248W, R175H and R273C, were among the mutations identified (see Table 4). The cases were categorised as follows: i) a group showing the LOF mutations or the above-mentioned hotspots ($n = 9$), ii) a *TP53* wild-type group ($n = 5$) and iii) a group consisting of unclassified *TP53* mutations ($n = 17$). The LOF and hotspot mutations were more commonly seen in the FIGO stage IV tumours ($p = 0.003$) and a low differentiation grade ($p = 0.024$).

The possible correlation of the *TP53* mutation status with PFS as a surrogate for response to chemotherapy was tested. The patients carrying tumours with the three groups of mutations showed a significantly different response to chemotherapy ($p = 0.029$), with the unclassified mutations revealing the longest PFS when compared to the wild-type and the LOF/hotspot patients. Similar results were found with the univariate survival analysis

Mutation	AA-change	Responder to Carboplatin n (%)	Non-Responder to carboplatin n (%)
7577545 T > C	M246V ^a	1 (4.8%)	0
7577579 G > C	R248W ^a	1 (4.8%)	1 (7.1%)
7578406 C > T	R175H ^a	0	1 (7.1%)
7574002 CG > C	FrameshiftR342*	1 (4.8%)	0
7578271 T > C	H193R ^a	1 (4.8%)	1 (7.1%)
7578190 T > C	Y220C ^a	0	1 (7.1%)
7577141 G > T	G266V ^a	1 (4.8%)	0
7577536 T > A	R249W ^a	1 (4.8%)	0
7577121 G > A	R273C ^a	0	1 (7.1%)
7577106 G > A	P278S ^a	1 (4.8%)	0
7577570 C > T	M237I ^a	1 (4.8%)	0
7577548 C > T	G245S ^a	1 (4.8%)	1 (7.1%)
7577577 T > C	N235S ^a	0	1 (7.1%)
7577509 C > A	E258Xnonsense ^{a*}	0	1 (7.1%)
7578535 T > C	K132R ^a	1 (4.8%)	0
7572990 CT > C	FrameshiftK373*	0	1 (7.1%)
7574017 C > A	R337L ^a	1 (4.8%)	0
7578527 A > C	C135G ^a	1 (4.8%)	0
7578210 T > C	R213R	1 (4.8%)	0
7579472 G > C	P72R ^a	2 (9.5%)	3 (21.4%)
7578271 T > A	H193L ^a	1 (4.8%)	0
7577556 C > G	C242S ^a	1 (4.8%)	0
7577121 GCAC > G	DeletionR273*	0	1 (7.1%)
7577122 C > G	V272V ^a	0	1 (7.1%)
7578529 A > C	F134C ^a	1 (4.8%)	0
7578442 T > G	Y163S ^a	1 (4.8%)	0
7578442 T > A	K120Xnonsense ^{a*}	1 (4.8%)	0

Table 4. Overview over mutations detected in our cohort. ^aMutation has been reported earlier in the IARC archive³⁹; *defined as hotspot or LOF mutation. Abbreviations: AA amino acid.

(logrank $p = 0.002$; Fig. 4C). When introducing a combined biomarker panel including the *TP53* mutation classes and levels of p53 isoforms into a Kaplan-Meier univariate model, we did not observe an enhanced discrimination between the patient groups (data not shown).

Discussion

The ability to predict response to first-line chemotherapy in HGSOC is currently limited. Better biomarkers are needed to optimise the therapeutic regimen for the patients. There are a limited number of studies assessing the prognostic relevance of the p53 network, including the aberrant expression of p53 isoforms reported in various human malignancies^{13–17,23–26,29,30}. By quantification of the mRNA levels of selected p53 isoforms in HGSOC tumour tissues, from patients carefully selected based on chemotherapy responses, we showed that the over-expression of the total $\Delta 133p53$ isoforms was associated with prolonged OS and PFS in multivariate survival analyses. However, the p53 isoform levels were not found to be significantly differentially distributed when the chemoresistant and chemosensitive cohorts were compared. These results are in line with a previous study that identified the $\Delta 133p53$ isoforms ($\Delta 133p53\alpha, \beta, \gamma$) as favourable prognostic factors in *TP53* mutated, advanced serous ovarian cancers²⁴. In contrast, $\Delta 133p53\beta$ has been shown to promote invasion and cancer cell stemness in breast cancer cell lines and has been associated with impaired survival in patients with breast carcinomas^{16,17}. The exact roles of $\Delta 133p53$ isoforms and the means by which they become tissue-specific therefore remain to be elucidated. Furthermore, the higher relative expression of p53 β to total p53 was associated with FIGO stage IIIC; thus, it could be hypothesised that p53 β plays a role in the metastatic potential. The p53 β isoform is missing the transactivation and tetramerization domains that seem necessary for enabling the transcriptional competence of p53³¹, and the higher expression has been associated with tumour traits and favourable survival in other cancer types^{15,29}.

The present data also revealed that the mRNA level of $\Delta 133p53$ was much higher than the levels of p53 β and p53 γ in most patients. This is in line with previous findings for uterine serous carcinomas²⁶. While the p53 β and p53 γ isoform may still be important, one may speculate that the low levels of these mRNAs compared to the total levels of p53 mRNA may limit their prognostic influence. We found expression levels of p53 isoforms to be highly correlated with each other. One possible explanation for this relationship is the presence of simultaneous alterations on both the amino- and carboxy-terminus of the protein. However, the isoform expression was not directly proportional to the total levels of p53 mRNA. It is therefore likely that isoforms are not merely a by-product of general p53 transcription but rather have their own biological importance. This controlled side-production of

isoforms by the splice machinery may reduce the wild-type transcript effect. Additionally, some of the cases analysed maybe possess a more general, inherent splice chaos.

The *TP53* mutation status had predictive significance when the *TP53* mutations were categorised into (i) a group with LOF mutations and common hotspots (R273, R248, R175) that was compared with the survival of patients bearing cancers (ii) with the *TP53* wild-type tumours or (iii) other, unclassified *TP53* defects. There are conflicting reports on the predictive value of different *TP53* mutation types in HGSOc^{6,7,32}. Similar to the findings in this study, other studies³³ have also found the PFS in patients with *TP53* wild-type tumours inferior to that of patients with non-canonical *TP53* mutations. Because *TP53* mutations are an almost universal observation in HGSOc⁴, the observed wild-type status could be questioned. It is possible that *TP53* is inactivated by alternative mechanisms in the patients with no detected *TP53* mutation.

A correlation was found between *TP53* LOF and hotspot mutations and the FIGO stage IV tumours. This is in line with previous studies revealing differential effects of the various *TP53* mutations. The *TP53* mutations seem to have a differential oncogenic capacity, depending on the mutation site and resulting downstream effect⁵. The univariate analyses of the combined biomarker panels for the *TP53* mutation classes and the expression of p53 isoforms did not enhance the significance of the prognostic information. This might have been the result of the small number of patients analysed in each group (n = 5–8; data not shown).

The clinical assessment of the *TP53* mutation status are regularly performed by immuno-histochemical staining³⁴. This standard diagnostic approach is based on the accumulation of p53 protein in a majority of *TP53* mutated cases. This accumulation of p53 protein is seen as the result of an increased protein stability of mutant p53. Here, we found that the *TP53* mutated specimens also had higher levels of total p53 mRNA, and this might have contributed to the resulting protein accumulation.

Notably, we found five patients to be *TP53* wild-type. While, there is an ongoing debate whether *TP53* mutations are ubiquitous in HGSOc, it is noteworthy that large sequencing efforts, such as TCGA, have also found a fraction of HGSOc to be *TP53* wild-type³³. As such we believe our findings regarding mutational status, represent the true biology of our cases.

The small number of cases resulting from the rigorous exclusion of possible confounders must be regarded as limitation of this study. In addition, the expression of the total $\Delta 40p53$ isoform was not detected in the current experiments although this isoform has been detected in comparable series²⁴. Although the current experimental setup enabled the quantitative detection of mRNAs containing the specific breakpoints for the different p53 isoforms, we were unable to reveal the combined breakpoints leading to alterations on both the carboxy-terminus and the amino-terminus (total $\Delta 133p53$ includes the pool of $\Delta 133p53\alpha$, $\Delta 133p53\beta$ and $\Delta 133p53\gamma$ isoforms). Currently, such mRNAs can be detected only qualitatively and, at best, semi-quantitatively. It is possible that isoform subtypes may possess an even better prognostic impact in HGSOc and other cancer types.

The ability to predict a good response to first-line chemotherapy in HGSOc is a crucial milestone in the implementation of personalised medicine. The term ‘BRCAness’ was introduced to describe ovarian or breast tumours that share molecular features and drug sensitivity with *BRCA*-mutated tumours³⁵. ‘BRCAness’ is associated with the response to PARP inhibitors, but no other molecular biomarkers play a role in the treatment stratification for HGSOc. The findings of this study point to the $\Delta 133p53$ isoform as a potential biomarker, pending further validation.

Methods

Patient characteristics. The original cohort of 493 individuals represents a consecutive collection of all of the patients diagnosed with and treated for EOC at Haukeland University Hospital, Bergen, Norway, during the period August 2001–June 2013. From this cohort, 40 patients with a good response to standard combination chemotherapy (‘responders’, defined as time to recurrence ≥ 17 months; n = 40) and 29 patients with a poor response to treatment (‘non-responders’, defined as progressive disease ≤ 6 months; n = 29) were selected to participate in the study. Advanced HGSOc was defined as FIGO stage IIIC or IV, high-grade (World Health Organization [WHO] Grade 2/3) serous histology and ovarian, primary peritoneal or fallopian origin. The patient demographic data and tumour traits, such as FIGO stage, as well as phenotypic characteristics, such as date of diagnosis and surgical treatment, level of complete cytoreduction and follow-up (at a mean of 41 months, range 2–144 months) were available for analysis (see Table 1).

All of the patients included in the study were treated with primary cytoreductive surgery and clinically staged according to the FIGO 2014 criteria³⁶. Surgical debulking was followed by platinum-based chemotherapy. Patients who were offered different treatment protocols, such as neoadjuvant chemotherapy and anti-angiogenic treatment, and patients who had concomitant cancers were excluded to avoid confounders. PFS was defined as the time interval, in months, between the date of the termination of adjuvant platinum-containing chemotherapy to the date of recurrence or last follow-up. OS was classified as an outcome measure and defined as the time interval, in months, from the day of the primary surgery to the last follow-up date or death from disease. Two patients were excluded from this part of the analysis because of missing follow-up data.

The study was conducted in accordance with the Declaration of Helsinki and approved by the local ethical committee (Regional Committees for Medical and Health Research Ethics Vest [REK], University of Bergen, Norway, id: 2018/72). The biological material and phenotypic data that formed the basis of this project are part of the Bergen Gynecologic Cancer Biobank, Women’s Clinic, Haukeland University Hospital, Bergen, Norway (REK id: 2014/1907 and 2015/548). In accordance with the local ethics committee’s guidelines, written informed consent was prospectively obtained from all of the women before the collection of fresh frozen tumour tissue, blood samples and clinicopathologic parameters was initiated.

Tumour tissue. After collection at the time of primary diagnosis, the tissue specimens were immediately frozen in liquid nitrogen, and the clinical data were annotated. If there were multiple eligible primary biopsies, the ovarian mass was the preferred tumour site for analysis. The tumour content of the fresh frozen specimens was assessed in ethanol-fixed and hematoxylin- and eosin- stained sections. While the minimum cut-off for inclusion was set at 50%, the tumour purity was more than 80% in a majority of the included tissue samples ($n = 39$). The histopathological analysis was performed at the Haukeland University Hospital Department of Pathology. The specimens were fixed in buffered formaldehyde, embedded in paraffin and further processed in the laboratory before standard histological sections were made. Pathologists trained in gynaecologic oncology performed the diagnostic assessments.

Nucleic acid isolation and cDNA synthesis. DNA was isolated from the fresh frozen samples by tissue digestion at 65 °C in a lysis buffer containing NaCl, EDTA 0.5 M pH8.5, TrisM pH8, sodium dodecyl sulphate (SDS) 5%, proteinase K 20 mg/ml and H₂O. Following overnight incubation, standard ethanol precipitation with sodium perchlorate and isopropanol was performed. DNA quantity was determined using a Qubit fluorometer (Thermo Fisher Scientific, Waltham, MA, USA). RNA was isolated using the RNeasy Mini Kit (Qiagen, Hilden, Germany) according to the manufacturer's instructions. RNA quantification was performed using a NanoDrop M-1000 spectrophotometer (Thermo Fisher Scientific, Waltham, MA, USA) and Agilent 2100 Bioanalyzer (Agilent Technologies, Santa Clara, CA, USA). A total of 500 ng RNA was added to 20 μ L reaction mix, and single-strand cDNA was synthesised using the Transcriptor Reverse Transcriptase system (Roche, Basel, Switzerland) according to the manufacturer's protocol.

Quantitative real-time PCR. Quantitative real-time PCRs (qPCR) were performed using specific primers and hydrolysis probes (see Table-S1) targeting total *TP53* or the different isoforms of *TP53*, as was previously described²⁶. Importantly, this experimental setup enabled the quantitative detection of the mRNA production of p53 isoforms; however, it did not allow for discrimination between the full-length molecules and their respective isoforms exhibiting alterations on both the carboxy-terminus and the amino-terminus. This important limitation is caused by the limited amplicon length used for the real-time qPCR. The mRNAs of the detected and quantified *TP53* were the total p53, total $\Delta 133$ p53, p53 β and p53 γ isoforms.

***TP53* sequencing and mutation calling.** The targeted massive parallel sequencing of the tumour DNA generated data on the *TP53* mutation status. The fragmentation of 1,000 ng dsDNA was achieved using the Covaris® M220 Focused-ultrasonicator™ (Covaris, Woburn, MA, USA). The library preparation was performed using the Agilent SureSelectXT reagent kit (Agilent Technologies, Santa Clara, CA, USA), and the individual samples were run on a MiSeq instrument (Illumina, San Diego, CA, USA). This design included +/-10 nucleotides at exon-intron borders, to cover potential splice site mutations. The *TP53* data was extracted from a sequencing effort applying baits targeting 360 genes as previously described in detail³⁷. Preliminary mutation calling was performed using the MiSeq Reporter (MSR) software, and the raw mutation calling output was revised by the application of post-processing filters. All of the suspected *TP53* mutations were validated by the manual inspection of the sequencing reads using the Integrative Genomics Viewer³⁸.

Statistical analyses. The Shapiro-Wilk test was performed to assess the normality assumption. On the basis of the non-normal distributed expression levels of total p53, total $\Delta 40$ p53, total $\Delta 133$ p53, p53 β and p53 γ isoforms, we calculated the Spearman's rank-order correlation for those variables. The Mann-Whitney U- and Kruskal-Wallis tests were applied to investigate the associations among the continuous variables (age and isoform expression levels) and the categorical variables (age grouped by median, disease stage, histological grade, presence of complete cytoreduction and chemoresistance as well as *TP53* mutation status). Fisher's exact test and Pearson's chi-squared test were used for comparisons of the categorical variables (patient age grouped by median, presence of complete cytoreduction, chemosensitivity and mutation status). The univariate survival analysis was performed by the Kaplan-Meier method, and subsets of patients (divided by median absolute or relative to total p53 expression of isoforms) were compared using the log-rank test. Multivariate survival analyses were performed using the Cox proportional-hazards regression model in a one-step fashion. Important clinical predictors of survival, such as age, FIGO stage and resection status, were added as categorical covariates. In the Cox proportional-hazards model, the absolute expression of the p53 isoforms and the isoform expression relative to the total p53 were tested as predictors. All of the *p*-values were reported as two-sided, and *p*-values < 0.05 were considered significant. The statistical analyses were performed using the SPSS 22.0 software package (SPSS Inc., Chicago, IL, United States of America).

Data Availability

The datasets generated during and/or analysed during the current study are available from the corresponding author on reasonable request.

References

1. Kandath, C. *et al.* Mutational landscape and significance across 12 major cancer types. *Nature*. **502**(7471), 333–339, <https://doi.org/10.1038/nature12634> (2013).
2. Patch, A. M. *et al.* Whole-genome characterization of chemoresistant ovarian cancer. *Nature*. **521**(7553), 489–94, <https://doi.org/10.1038/nature14410> (2015).
3. Cancer Genome Atlas Research Network. Integrated genomic analyses of ovarian carcinoma. *Nature*. **474**(7353), 609–15, <https://doi.org/10.1038/nature10166> (2011).
4. Ahmed, A. A. *et al.* Driver mutations in TP53 are ubiquitous in high grade serous carcinoma of the ovary. *J Pathol*. **221**(1), 49–56, <https://doi.org/10.1002/path.2696> (2010).

5. Brosh, R. & Rotter, V. When mutants gain new powers: news from the mutant p53 field. *Nat Rev Cancer*. **9**(10), 701–13, <https://doi.org/10.1038/nrc2693> (2009).
6. Seagle, B. L. *et al.* Survival of patients with structurally-grouped TP53 mutations in ovarian and breast cancers. *Oncotarget*. **6**(21), 18641–52, <https://doi.org/10.18632/oncotarget.4080> (2015).
7. Seagle, B. L. *et al.* TP53 hot spot mutations in ovarian cancer: selective resistance to microtubule stabilizers *in vitro* and differential survival outcomes from The Cancer Genome Atlas. *Gynecol Oncol*. **138**(1), 159–64, <https://doi.org/10.1016/j.ygyno.2015.04.039> (2015).
8. Brachova, P. *et al.* TP53 oncomorphic mutations predict resistance to platinum and taxanebased standard chemotherapy in patients diagnosed with advanced serous ovarian carcinoma. *Int J Oncol*. **46**(2), 607–18, <https://doi.org/10.3892/ijo.2014.2747> (2015).
9. Kobel, M. *et al.* The biological and clinical value of p53 expression in pelvic high-grade serous carcinomas. *J Pathol*. **222**(2), 191–8, <https://doi.org/10.1002/path.2744> (2010).
10. Fransson, A. *et al.* Strong synergy with APR-246 and DNA-damaging drugs in primary cancer cells from patients with TP53 mutant high-Grade Serous ovarian cancer. *J Ovarian Res*. **9**(1), 27, <https://doi.org/10.1186/s13048-016-0239-6> (2016).
11. Mohell, N. *et al.* APR-246 overcomes resistance to cisplatin and doxorubicin in ovarian cancer cells. *Cell Death Dis*. **6**, e1794, <https://doi.org/10.1038/cddis.2015.143> (2015).
12. Surget, S., Khoury, M. P. & Bourdon, J. C. Uncovering the role of p53 splice variants in human malignancy: a clinical perspective. *Oncotargets Ther*. **7**, 57–68, <https://doi.org/10.2147/OTT.S53876> (2013).
13. Fujita, K. *et al.* p53 isoforms Delta133p53 and p53beta are endogenous regulators of replicative cellular senescence. *Nat Cell Biol*. **11**(9), 1135–42, <https://doi.org/10.1038/ncb1928> (2009).
14. Silden, E. *et al.* Expression of TP53 isoforms p53beta or p53gamma enhances chemosensitivity in TP53(null) cell lines. *PLoS One*. **8**(2), e56276, <https://doi.org/10.1371/journal.pone.0056276> (2013).
15. Anensen, N. *et al.* Correlation analysis of p53 protein isoforms with NPM1/FLT3 mutations and therapy response in acute myeloid leukemia. *Oncogene*. **31**(12), 1533–45, <https://doi.org/10.1038/ncr.2011.348> (2012).
16. Arsic, N. *et al.* The p53 isoform Delta133p53beta promotes cancer stem cell potential. *Stem Cell Reports*. **4**(4), 531–40, <https://doi.org/10.1016/j.stemcr.2015.02.001> (2015).
17. Gadea, G. *et al.* TP53 drives invasion through expression of its Delta133p53beta variant. *Elife*. **5**, <https://doi.org/10.7554/eLife.14734> (2016).
18. Khoury, M. P. & Bourdon, J. C. The isoforms of the p53 protein. *Cold Spring Harb Perspect Biol*. **2**(3), a000927, <https://doi.org/10.1101/cshperspect.a000927> (2010).
19. Graupner, V., Schulze-Osthoff, K., Essmann, F. & Janicke, R. U. Functional characterization of p53beta and p53gamma, two isoforms of the tumor suppressor p53. *Cell Cycle*. **8**(8), 1238–48, <https://doi.org/10.4161/cc.8.8.8251> (2009).
20. Marcel, V. *et al.* Biological functions of p53 isoforms through evolution: lessons from animal and cellular models. *Cell Death Differ*. **18**(12), 1815–24, <https://doi.org/10.1038/cdd.2011.120> (2011).
21. Solomon, H., Sharon, M. & Rotter, V. Modulation of alternative splicing contributes to cancer development: focusing on p53 isoforms, p53beta and p53gamma. *Cell Death Differ*. **21**(9), 1347–9, <https://doi.org/10.1038/cdd.2014.99> (2014).
22. Bourdon, J. C. *et al.* p53 isoforms can regulate p53 transcriptional activity. *Genes Dev*. **19**(18), 2122–37, <https://doi.org/10.1101/gad.1339905> (2005).
23. Hofstetter, G. *et al.* The N-terminally truncated p53 isoform Delta40p53 influences prognosis in mucinous ovarian cancer. *Int J Gynecol Cancer*. **22**(3), 372–9, <https://doi.org/10.1097/JGCO.0b013e31823ca031> (2012).
24. Hofstetter, G. *et al.* Delta133p53 is an independent prognostic marker in p53 mutant advanced serous ovarian cancer. *Br J Cancer*. **105**(10), 1593–9, <https://doi.org/10.1038/bjc.2011.433> (2011).
25. Hofstetter, G. *et al.* Alternative splicing of p53 and p73: the novel p53 splice variant p53delta is an independent prognostic marker in ovarian cancer. *Oncogene*. **29**(13), 1997–2004, <https://doi.org/10.1038/ncr.2009.482> (2010).
26. Bischof, K. *et al.* High expression of the p53 isoform gamma is associated with reduced progression-free survival in uterine serous carcinoma. *BMC Cancer*. **18**, 684, <https://doi.org/10.1186/s12885-018-4591-3> (2018).
27. Schwarz, R. F. *et al.* Spatial and temporal heterogeneity in high-grade serous ovarian cancer: a phylogenetic analysis. *PLoS Med*. **12**(2), e1001789, <https://doi.org/10.1371/journal.pmed.1001789> (2015).
28. McGranahan, N. & Swanton, C. Biological and Therapeutic Impact of Intratumor Heterogeneity in Cancer Evolution. *Cancer Cell*. **27**(1), 15–26, <https://doi.org/10.1016/j.ccell.2014.12.001> (2015).
29. Avery-Kiejda, K. A., Morten, B., Wong-Brown, M. W., Mathe, A. & Scott, R. J. The relative mRNA expression of p53 isoforms in breast cancer is associated with clinical features and outcome. *Carcinogenesis* **35**(3), 586–96, <https://doi.org/10.1093/carcin/bgt411> (2014).
30. Bourdon, J. C. *et al.* p53 mutant breast cancer patients expressing p53gamma have as good a prognosis as wild-type p53 breast cancer patients. *Breast Cancer Res*. **13**(1), R7, <https://doi.org/10.1186/bcr2811> (2011).
31. Janicke, R. U., Graupner, V., Budach, W. & Essmann, F. The do's and don'ts of p53 isoforms. *Biol Chem*. **390**(10), 951–63, <https://doi.org/10.1515/BC.2009.093> (2009).
32. Kang, H. J., Chun, S. M., Kim, K. R., Sohn, I. & Sung, C. O. Clinical relevance of gain-of-function mutations of p53 in high-grade serous ovarian carcinoma. *PLoS One*. **8**(8), e72609, <https://doi.org/10.1371/journal.pone.0072609> (2013).
33. Wong, K. K. *et al.* Poor survival with wild-type TP53 ovarian cancer? *Gynecol Oncol* **130**(3), 565–9, <https://doi.org/10.1016/j.ygyno.2013.06.016> (2013).
34. Kobel, M. *et al.* Optimized p53 immunohistochemistry is an accurate predictor of TP53 mutation in ovarian carcinoma. *J Pathol Clin Res*. **13**(2(4)), 247–258, <https://doi.org/10.1002/cjp.2.53> (2016).
35. Lord, C. J. & Ashworth, A. BRCAness revisited. *Nat Rev Cancer*. **16**(2), 110–20, <https://doi.org/10.1038/nrc.2015.21> (2016).
36. Prat, J. & FIGO Committee on Gynecologic Oncology. Staging classification for cancer of the ovary, fallopian tube, and peritoneum. *Int J Gynaecol Obstet*. **124**(1), 1–5, <https://doi.org/10.1016/j.ijgo.2013.10.001> (2014).
37. Yates, L. R. *et al.* Subclonal diversification of primary breast cancer revealed by multiregion sequencing. *Nat Med*. **21**(7), 751–9, <https://doi.org/10.1038/nm.3886> (2015).
38. Robinson, J. T. *et al.* Integrative genomics viewer. *Nat Biotechnol*. **9**(1), 24–6, <https://doi.org/10.1038/nbt.1754> (2011).
39. Bouaouin, L. *et al.* TP53 Variations in Human Cancers: New Lessons from the IARC TP53 Database and Genomics Data. *Hum Mutat*. **37**(9), 865–76, <https://doi.org/10.1002/humu.23035> (2016).

Acknowledgements

This work was supported by grants from The Western Norway Regional Health Authority (Project No. 911809 and 911852) and the Research Council of Norway project no. 239837. We thank Britt Irene Edvardsen, Reidun Kopperud, Kadri Madissoo and Beryl Leirvaag for technical assistance.

Author Contributions

Conceptualization, K.B., S.K., H.B.S., B.T.G. and L.B.; methodology, K.B., S.K. and S.M.H.; formal analysis, K.B. and S.M.H.; investigation, I.S. and K.W.; resources, I.S. and K.W.; data curation, K.B.; writing – original draft preparation, K.B.; writing – review and editing, S.K., S.M.H. and L.B.; supervision, B.T.G. and L.B.; project administration, L.B.; funding acquisition, L.B.

Additional Information

Supplementary information accompanies this paper at <https://doi.org/10.1038/s41598-019-41706-z>.

Competing Interests: The authors declare no conflicts of interest.

Publisher's note: Springer Nature remains neutral with regard to jurisdictional claims in published maps and institutional affiliations.



Open Access This article is licensed under a Creative Commons Attribution 4.0 International License, which permits use, sharing, adaptation, distribution and reproduction in any medium or format, as long as you give appropriate credit to the original author(s) and the source, provide a link to the Creative Commons license, and indicate if changes were made. The images or other third party material in this article are included in the article's Creative Commons license, unless indicated otherwise in a credit line to the material. If material is not included in the article's Creative Commons license and your intended use is not permitted by statutory regulation or exceeds the permitted use, you will need to obtain permission directly from the copyright holder. To view a copy of this license, visit <http://creativecommons.org/licenses/by/4.0/>.

© The Author(s) 2019